Environmental and economic sustainability of crack mitigation in reinforced concrete with SuperAbsorbent Polymers (SAPs)

Davide di Summa[1,3] , José Roberto Tenório Filho[1, 5], Didier Snoeck[2], Philip Van den Heede[1], Sandra Van Vlierberghe[3], Liberato Ferrara[4] , Nele De Belie[1].

1. Ghent University, Department of Structural Engineering and Building Materials; Magnel-Vandepitte Laboratory, Tech Lane Ghent Science Park, Campus A, Technologiepark Zwijnaarde 60, B-9052 Ghent, Belgium;
Davide.diSumma@UGent.be; Roberto.Tenorio@UGent.be; Philip.VandenHeede@UGent.be;
Nele.DeBelie@UGent.be

2. BATir, Université Libre de Bruxelles (ULB), 50 av F.D. Roosevelt, CP 194/02, B-1050, Brussels, Belgium
Didier.Snoeck@Ulb.be

3. Ghent University, Department of Organic and Macromolecular Chemistry, Centre of Macromolecular Chemistry, Polymer Chemistry & Biomaterials Group, Krijgslaan 281,S4 9000 Ghent, Belgium;
Sandra.VanVlierberghe@UGent.be

4. Politecnico di Milano, Department of Civil and Environmental Engineering, piazza Leonardo da Vinci 32, 20133 Milan, Italy;
Liberato.Ferrara@PoliMi.it

5. SIM vzw, Technologiepark Zwijnaarde 48, B-9052 Ghent, Belgium

Abstract

Due to the increasing awareness and sensitivity towards the environmental and economic sustainability issues, the concrete industry has to deliver innovative solutions, in terms of materials, products and structural concepts, to achieve higher durability of engineering feats in real service scenarios. The inclusion of SuperAbsorbent Polymers (SAPs) into the concrete mix, can not only stimulate the autogenous crack healing, but is also able to reduce the shrinkage cracking through internal curing. In this paper, Life Cycle Assessment (LCA) and Life Cycle Cost (LCC) analysis have been performed to assess both the ecological and economic profile, in real scale, of conventional reinforced concrete structures, made with concrete containing SAPs, in comparison to a reference solution without any addition. For this purpose, the corrosion of reinforcement has been regarded as the main degradation mechanism and different corrosion models have been considered and combined with the structural analysis principles to obtain reliable Service Life (SL) estimations. Four different scenarios, with a SL ranging from 50 up to 100 years, have been analyzed to assess the potential benefits of a wall, cast with SAP-containing concrete (Wall_SAP). Both Wall_SAP and a reference wall without SAP (Wall_Ref) are subjected to the concrete cover replacement as main maintenance activity while for the Wall_Ref also the crack filling by means of polyurethane resin is considered as an option (Wall_Resin). The adopted CML impact-assessment method, developed by the Center of Environmental Science of Leiden University, shows the advantage of using SAPs, since the

environmental burdens were reduced up to 20% in the case of Fresh Water Aquatic Ecotoxicity impact category in comparison to the reference for the fourth scenario. In this scenario a hemispherical corrosion pit model for the steel bars and a service life of 100 years were taken into account. Furthermore, the economic assessment developed for the same scenario, pointed out for the SAPs based solution, there identified as Wall_SAP_M2_100, a consistent reduction in terms of costs up to 14% if compared to the reference, there named as Wall_Ref_M2_100. The outcomes definitely highlight the potential of the analyzed technology that can fulfil the future needs of the stakeholders involved in the construction sector.

Keywords: LCA, LCC, Sustainability, Concrete, Self-Healing, SAPs

1 Introduction

Concrete is the most widely used construction material worldwide due to its structural characteristics, low cost, ease of production and casting procedures and endless shaping possibilities. However, according to the foreseen growth in its use, and as a part of the increasing awareness and consciousness for sustainability of the construction industry as a whole, its environmental and economic sustainability performance need to be addressed in a proper framework and from a holistic perspective (design-wise). The cement production itself yields about 800 kg of CO_2 per ton of cement released into the atmosphere and uses large shares of non-renewable raw resources, including natural rocks and water (Meyer, 2009)(Federico and Chidiac, 2009). Additionally, considering the structural service scenario, concrete is generally characterized by a high cracking susceptibility, cracks representing a preferential ingress-path for harmful substances from outdoor environment, accelerating the corrosion process of the reinforcement and the related concrete degradation (Belleghem et al., 2017). As a matter of fact, concrete durability is a critical issue with environmental, economic and social impacts on society. The deterioration of concrete structures requires continuous maintenance and repairing activities, that generally imply the removal and the disposal of the damaged reinforcement and concrete, with the consequent need of new raw materials, energy and workmanship to restore the integrity and the pristine level of performance of the structure. Related expenditures also have to be taken into consideration. Recently researchers have been developing innovative materials that can represent a solution in this respect, taking advantage of specific mechanisms that ensure the self-repair of cracks upon occurrence, hence improving the durability of the structure (Liu et al., 2021)(Plank et al., 2015)(Craeye et al., 2011a)(Feiteira et al., 2016)(Gruyaert et al., 2016)(Pelto et al., 2017). As example of that, SuperAbsorbent Polymers (SAPs), blended into the concrete matrix, represent an interesting technology. SAPs are a natural or synthetic water-insoluble 3D network of polymeric chains cross-linked by chemical or physical bonding. They possess the ability to take up a significant amount of fluids (up to 1500 times their own weight) (Mechtcherine and Reinhardt, 2012). The initial water uptake, swelling, and the later gradual water release are of great interest in the development of more durable cementitious materials. Once in contact with the mixing water of the fresh cementitious matrix, SAPs absorb and retain a certain amount of the water (depending on their absorption capacity), later on acting as water reservoirs for the system, able to keep high levels of internal relative humidity for a considerable time frame. Because of that feature, over the past two decades, SAPs have been used in cementitious materials for the purposes of internal curing to prevent shrinkage-cracking due to self-desiccation (Piérard et al., 2006)(Snoeck et al., 2015)(Craeye et al., 2011b). Additionally, SAPs can promote the immediate sealing of cracks: upon cracking, the water that penetrates the cracks is generally absorbed by the SAPs that expand in volume, blocking the crack and preventing further entry of water and harmful substances (Snoeck et al., 2012).

Then, in time, the captured water is released again stimulating the hydration of unhydrated binder materials (when present) resulting in autogenous healing of the crack (Snoeck et al., 2014). Nevertheless, this kind of innovations usually face several barriers in their use, mainly due to the lack of information and to the possible higher initial investment cost. Hence, Life Cycle Assessment (LCA) and Life Cycle Cost (LCC) analysis are the tools to be adopted to lead design decisions throughout the entire design process. For a SAP-containing concrete, the use of 1 wt% by binder of SAP to favor the autogenous crack healing, together with 2 vol% of polypropylene microfibers, specifically employed to ensure a multiple cracking behavior in a concrete matrix based on Portland cement and including fly ash, silica sand, water and poly-carboxyl ether-based superplasticizer, was already investigated (Van den Heede et al., 2018). The work, selecting as functional unit (FU) a slab (5 m large, 1 m wide and 0.17 m thick) with a service life of 100 years, highlighted that the investigated advanced cementitious composites allow to reduce around 60% the environmental impacts in comparison to Portland cement concrete solutions (Van den Heede et al., 2018). Despite the literature which is continuously growing in this field, the previous work still represents the only one that applied LCA to assess environmental impacts related to the use of SAPs on a large-scale structure. Therefore, the scope of this paper, is to further address the possible benefits from the environmental and the economical point of view. This was done developing also a Life Cycle Cost (LCC) analysis to assess the potential economic viability of these polymers, as "non-conventional" concrete constituents in a real structural service scenario. To this purpose, reference will be made to a case study consisting of two mock-up walls casted in Bruges (Belgium), intended to replicate a tunnel segment element, also to demonstrate and foster the feasibility of employing these advanced materials on a large scale industrial basis.

2 Case study

The case study consisted of two earth-retaining walls intended to replicate tunnel segment elements. Both "walls" are 14 m long, 2.75 m high and have a 0.80 m deep cross section. One of them, henceforth indicated as Wall_Ref, was produced with concrete C35/45 and reinforced on either side with horizontal Φ16 mm steel bars spaced at 96 mm and vertical Φ12 mm reinforcement bars spaced at 140 mm. The second wall, denoted as Wall_SAP, was produced with concrete C30/37, containing the same amount of vertical Φ12 steel bars with a reduced quantity of longitudinal Φ16 mm bars spaced at 107 mm instead of 96 mm as done for Wall_Ref. The reinforcement of both walls was designed to allow a maximum crack width of 300 μm. In fact, given the difference in the strength class and considering that the internal curing promoted by the SAPs could counteract the shrinkage-deformation and hence mitigate the restrained shrinkage-cracking, both walls have been designed expecting the same cracking pattern, even with a reduction in the reinforcement for Wall_SAP. Additionally, the walls were built on two foundation slabs casted at least three months prior to the walls and made with the same concrete of Wall_Ref. As it is possible to observe in Table 1, which details the two adopted mix designs, Wall_SAP contains a higher water-to-cement ratio since it includes both the effective mixing water and the entrained water in the SAPs. However, it is important to highlight that the entrained water in the SAPs is considered only for the purpose of internal curing, thus, it is also possible to affirm that both concrete mixtures have the same effective water-to-cement ratio. The walls have been cast in the framework of the iSAP project, in which innovative superabsorbent polymers were used for the production of smart concrete mixtures, designed to possess the features of internal curing, self-sealing and self-healing of cracks. It was shown that the thereby developed innovative SAPs added to the concrete mixture were even more efficient in crack mitigation than expected and no cracks were noticed over the complete monitoring period of 9 months (Tenório Filho et al., 2021a) differently from

the reference structure where, as shown in Fig. 1, several cracks were already observed. In previous laboratory experiments it was furthermore shown that this concrete mixture had the potential to

***Table 1**:* Wall_Ref and Wall_SAP mix design per 1 m³

	Wall_Ref [kg]	**Wall_SAP [kg]**
CEM III-B 42.5N	359.78	359.82
Limestone 2/20	1,124.44	1,084.55
Marine sand 0/4	782.22	744.55
Superplasticizer Sika ViscoFlow-26	1.56	1.55
Superplasticizer Tixo	2.42	2.42
Water	114.44	137.45
Commercial SAP	-	1.36

reduce water permeability through cracks of up to 250 µm in width, and increase the resistance to salt-scaling under frost attack with a limited reduction in the compressive strength (Tenório Filho et al., 2021a)(Tenório Filho et al., 2020a)(Tenório Filho et al., 2020b)(Tenório Filho et al., 2019)(Tenório Filho et al., 2021b).

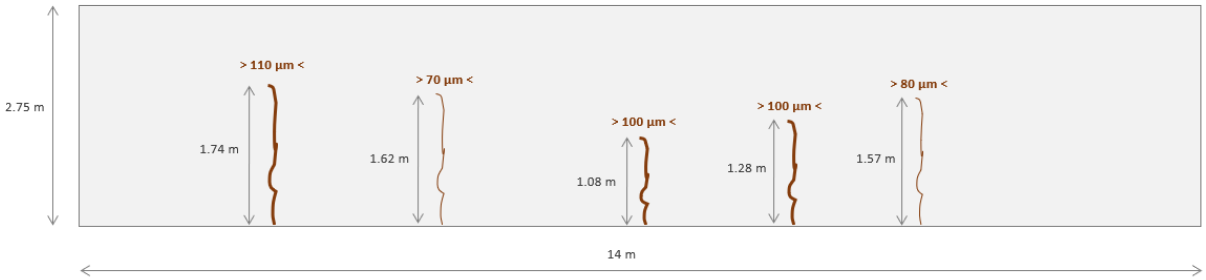

Figure 1: Cracking pattern of the reference wall at the age of 30 days. Adapted from *(Tenório Filho, 2021a)*

3 Concrete walls repair

Nowadays, several methods are available to restore the functionality of damaged concrete structures, with a broad variety of materials and technologies to be used according to the occurred damage. However, it should be emphasized that the design phase of a given structure already takes into account the minimum "deemed to satisfy" requirements to ensure an adequate durability according to the boundary conditions. For instance, current codes and regulations, e.g. Eurocode 2 (CEN, 2005a), identify three measures to protect the steel reinforcement: limitation of the crack width, adequate concrete cover and appropriate concrete quality, achieved through minimum compressive strength and cement content, and maximum water-to-cement ratio. Additionally, EN 1504 (CEN, 2005b) defines the procedures and the characteristics of the products to repair the concrete structures. The standard is divided into ten parts, where the ninth describes eleven principles in total, defining for each one a specific prevention or repair activity. These range from hydrophobic impregnation to control the humidity, casting of new concrete layers to restore the damaged sections, substitution of reinforcement bars or post-tensioning of the existing ones to ensure the stability of the structure, up

to the application of an electric potential to realize cathodic protection. Therefore, the commercially available materials that could be used for this purpose are various but, as easily understandable, each solution will result into different environmental impacts. This paper investigates the concrete cover replacement with the substitution of the damaged reinforcement bars as the main conventional technique to restore the functionality of Wall_Ref. This intervention would be needed from the moment when preferential penetration of chlorides or carbonation along the cracks will result into unacceptable damage to the reinforcement that would impair the structural stability. This choice is also supported by the work of Tilly and Jacobs (Tilly and Jacobs, 2007) who developed an international survey of which the results were already used in similar LCA researches (Van den Heede et al., 2018) highlighting that the concrete cover repairing technique had been used in 60% of the surveyed cases. Additionally, as these results could not be exhaustive, also polyurethane resin injection by pressure was assessed as repair technique for the purpose of this research, commonly applied in Belgium for repairing cracks occurring in tunnel elements.

3.1 Concrete cover and reinforcement substitution

According to the carbonation and chloride corrosion mechanisms, after the initiation time, the volumetric expansion of the corrosion products causes cracks along the concrete cover up to its spalling. Various experimental studies have been carried out to address the radial expansion of corroded reinforcement and its effects on concrete structures (Andrade et al., 1996)(Liu and Weyers,1998)(Clark and Saifullah, 1993)(Al-Sulaimani et al., 1990)(Rasheeduzzafar et al., 1992)(Williamson and Clark, 2000). Generally, a common adopted technique to restore the functionality of a concrete structure, consists of the mechanical removal of the concrete cover, the substitution of the damaged reinforcement bars and the casting of a new concrete layer after a prior treatment with an epoxy-based product to ensure a better adhesion to the substrate. A key research focus, in view of the aforementioned discussion, is to determine when the reduced structural stability due to the reinforcement corrosion, will require the demolition of the concrete cover to replace the damaged bars for both Wall_Ref and Wall_SAP. The following sections better detail the approach here used, whose results are employed to define the 4 different scenarios in which the functional unit (FU) is assessed for the scope of this research. More specifically, while Scenario 1 and Scenario 2 assess a uniform corrosion propagation rate presented in 3.1.4, Scenario 3 and 4 take into account a more severe condition with a localized corrosion area as detailed in 3.1.5. Furthermore, Scenario 1 and 3 are limited to 50 years of SL, while Scenario 2 and 4 are aiming at 100 years.

3.1.1 Structure stability

Since the walls are comparable to earth-retaining walls designed for tunnel applications, it is possible to calculate the lateral earth pressure using the Coulomb theory as in Eq. [1].

$$S = \frac{\gamma_t}{2} \times H^2 \times tg^2\left(\frac{90 - \varphi}{2}\right) \qquad \text{Eq. [1]}$$

where, H is the height of the structure while γ_t and φ are the specific weight and the internal friction coefficient of a saline soil, assumed respectively equal to 18 kN/m^3 and 35° according to the literature. As shown in **Figure 3**, a cantilever model was employed to design the structure and to calculate the bending moment action due to the soil thrust which has to be resisted through the moment resisting capacity of the wall base cross section.

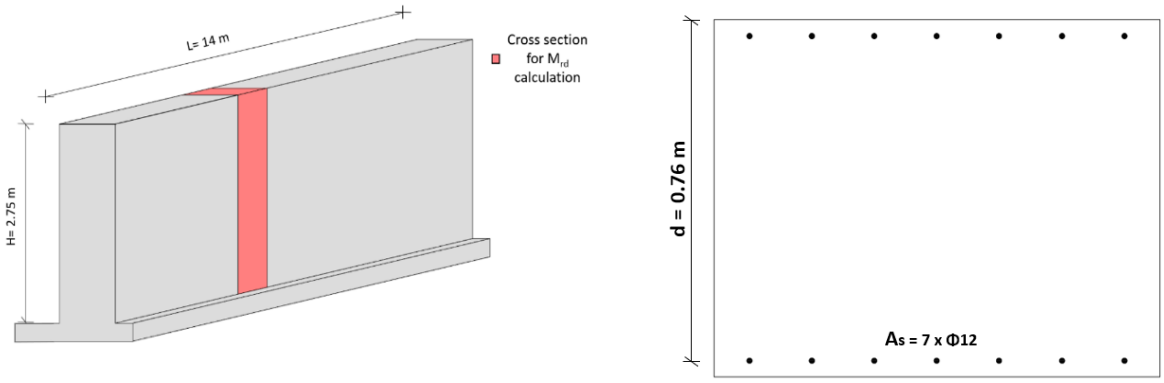

***Figure 2**: Three-dimensional view of the wall (on the left) and horizontal cross section (on the right) considered to calculate M_{Rd}*

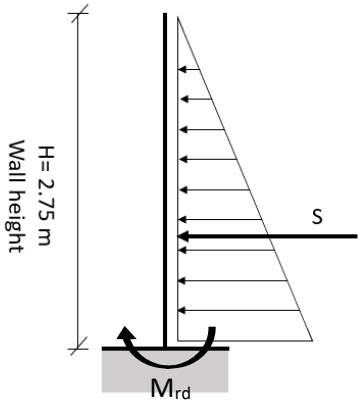

Figure 3: Model used for calculations

Therefore, using Eq. [1], it is possible to calculate, for a 1 m long strip of the wall, a total earth thrust equal to 18.44 kN/m applied at H/3, which corresponds to a bending moment equal to 16.90 kNm/m. The latter, was then amplified by a coefficient γ_G of 1.35 as per EN 1990:2002, with a resultant bending moment design value (M_{Ed}) equal to 22.82 kNm/m. Eq. [2] was then adopted to estimate the resistant moment $M_{Rd,}$ equal to 212.9 kNm. According to the cross section of the wall presented in Figure 2, a value of 391.3 N/mm^2 was used for the design yielding strength of steel f_{yd}, calculated from the characteristic yield stress f_{yk} of a B450C steel, while 791 mm^2 and 764 mm were used for the tension reinforcement bar area A_s and the effective depth d, respectively.

$$M_{rd} = 0.9 \cdot f_{yd} \cdot A_S \cdot d \qquad \text{Eq. [2]}$$

Since the wall is designed as part of a tunnel, the weight of the wall itself should also been taken into account for the M_{Rd} calculations. However, since for the considered 1 m long strip, it is equal to about 55 kN/m (less than 1% of the axial load capacity of the base cross section), it can be regarded as negligible for the scope of this research, not significantly affecting the final results.

Therefore, since it must be always verified that $M_{Ed} < M_{Rd}$, it is easily possible to calculate that the A_s value must be higher than 8483 mm^2. This means that, as in one meter of the wall 7 Φ12 mm bars are located, assuming the same corrosion progress along the entire wall, each reinforcement bar cannot lose more than 89% of its cross-section. The reduced A_s values imply that the safety of the structure

cannot be ensured any longer and specific repairing activities must be adopted to reinstate an acceptable A_s value.

3.1.2 Corrosion initiation

Before calculating how long it would take chloride-induced corrosion to affect the load bearing capacity of the structure, it is necessary to calculate the time the chloride ions will need to penetrate the concrete matrix and reach a critical concentration value at the cover depth, i.e. at the level of the most external surface of the reinforcement. To this purpose, the 2nd Fick law presented in Eq. [3] is generally employed.

$$x_{crit} = 2\sqrt{3(t - t_0) \cdot D_{app}} \cdot \left[1 - \sqrt{\frac{(C_{crit} - C_I)}{C_s - C_i}}\right] \quad \text{Eq. [3]}$$

Where x_{crit} is the critical chloride depth assumed equal to the concrete cover, C_i is the initial chloride content of concrete equal to 0.20% by weight of cement according to EN 206 (CEN, 2016); C_s is the chloride concentration at the surface being 0.92% by weight of soil for the case of saline soil (Regione Emilia Romagna, 2011) and C_{crit} is the critical chloride concentration equal to 0.44% by weight of cement according to Alonso et al. (Alonso and Sanchez, 2009) and based on field exposure tests developed for the specific purpose. D_{app} is the apparent chloride diffusion coefficient whose values, as better detailed in 3.1.3, may range from 10^{-10} m^2/s to 10^{-12} m^2/s.

3.1.3 The incidence of D_{app} values for both LCA and LCC calculations

With regard to the D_{app} value, the currently available literature does not give any detail about the effect of SAP addition. A value of 10^{-10} m^2/s is generally reported for the case of cracked concrete while for the uncracked one, containing CEM I, a value one order of magnitude smaller could be used, equal to 10^{-11} m^2/s (Al-Obaidi et al., 2020)(Shafikhani and Chidiac, 2019)(Torres-Acosta et al., 2019)(Liu et al., 2015). Additionally, since Wall_SAP contains CEM III/B, a theoretical correction factor of 0.2 according to (Coppola, 2007) allows to pass from 10^{-11} m^2/s value to a resulting 10^{-12} m^2/s (as the order of magnitude). According to this, an initiation time of almost 0 was calculated for the cracked Wall_Ref (corresponding to the wall itself prior to any other maintenance activity) using 10^{-10} m^2/s. In contrast, a D_{app} value equal to 10^{-12} m^2/s has been used for Wall_Ref after having received the first maintenance activity and for Wall_SAP. This resulted into a corrosion initiation time of 13 years in total. This could be assumed, considering that no cracks were observed up to 9 months after casting for the Wall_SAP and no cracks are supposed for Wall_Ref after its restoration until when the chloride will reach the reinforcement surface causing the steel corrosion. These different initiation times clearly express the need to integrate the structural properties of a given structure into the LCA and LCC evaluations. As a matter of fact, different D_{app} values lead to clearly different initiation times, passing from around 0 years when assuming a value of 10^{-10} m^2/s, through 1 year when using 10^{-11} m^2/s up to 13 years in total with 10^{-12} m^2/s. Therefore, since a longer initiation period corresponds to a more delayed corrosion of the steel bars with a resulting different frequency of the maintenance activities, the more precise the structural considerations will be, the more accurate the LCA and LCC will be.

3.1.4 Corrosion propagation - rates from the literature

When water and oxygen are present on the surface of the reinforcement, the corrosion occurs with a rate that could be expressed as penetration rate in µm/y. Some authors (Bertolini et al., 2004) distinguish among a negligible rate lower than 2 µm/year, a low rate between 2 and 5 µm/year, a

moderate rate between 5 and 10 µm/year, an intermediate rate between 10 and 50 µm/year, a high rate between 50 and 100 µm/year and a very high rate above 100 µm/year. More specifically, for a concrete contaminated by chloride and subjected to 80-90% of relative humidity (RH), the closest assumption to the case studies of this research, the corrosion rate can vary from 10 µm/year up to 50 µm/year (Bertolini et al., 2004). Therefore, taking into account the most severe condition equal to 50 µm/year after the initiation period, it is possible to estimate a propagation time for a Φ12 mm rebar system as in Fig 4.

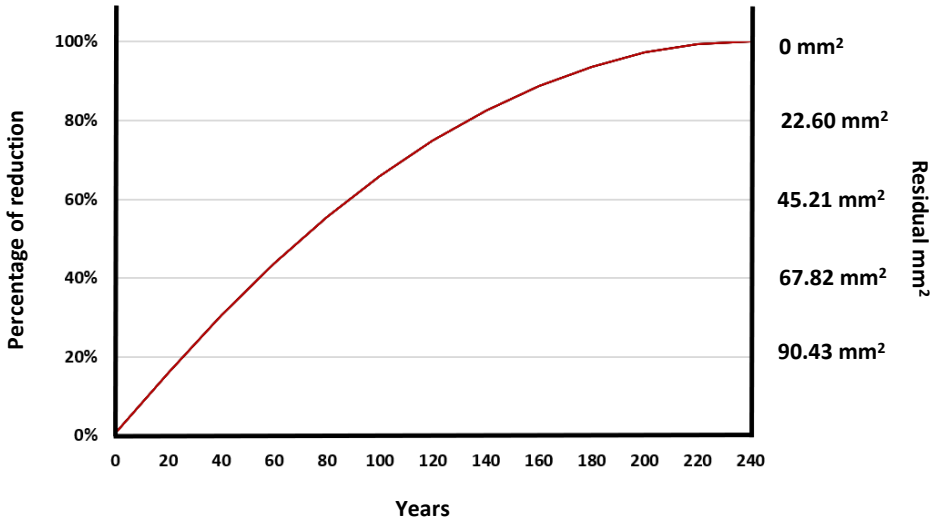

***Figure 4**: Percentage of cross area reduction for Φ12 bars, assuming* 50 µm/year, *according to* (Bertolini et al. 2004).

3.1.5 Corrosion propagation – hemispherical pit calculation

Differently from the previous case, that basically considers a uniform corrosion of the steel reinforcement, it is possible to assume that chloride induced corrosion is restricted to a very localized damage. This means that the mass (and volume) loss of steel is concentrated in a small zone (pit corrosion) that increases as the corrosion propagates in time, generating a volumetric mass loss of the steel, as shown in **Figure 55**. However, this still represents a simplified approach since the corrosion itself also implies the build-up of expansive corrosion products at the rebar surface with a consequent concrete cover cracking which will favor the ingress of further chlorides, here not taken into account. The volume and the area of the pit are calculated as stated by Van Belleghem (Van Belleghem, 2018), using the Eq. [4] and Eq.[5].

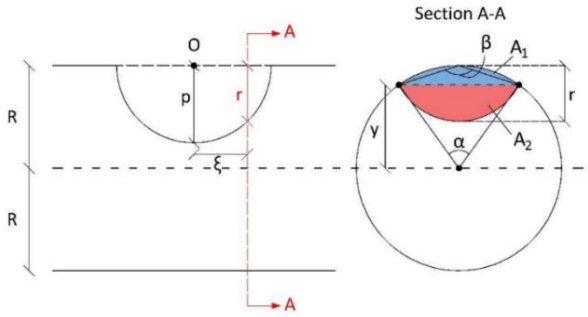

***Figure 5**:* Schematic representation of the hemispherical pit model as detailed in (Van Belleghem, 2018)

Table 2: Calculated area and volume of the hemispherical pit

p (mm)	V_{pit} (mm^3)	A_{loss} (mm^2)	A_{loss} (%)	Years to develop corrosion pit
1	**2.03**	**1.52**	**1**	**0.4**
2	15.71	5.84	5	0.5
3	51.22	12.63	11	1.6
4	117.13	21.54	19	3.8
5	220.27	32.20	28	7.2
6	365.66	44.22	39	12
7	556.28	57.18	51	18.3
8	792.78	70.59	62	26.1
9	1073.01	83.88	74	35.3
10	1391.16	96.33	85	45.8
11	1735.81	106.87	95	57.2
12	2083.11	113.10	100	68.7

$$A_{pit} = A_1 + A_2 = \frac{R^2}{2} \cdot (\alpha - \sin\alpha) + \frac{r^2}{2} \cdot (\beta - \sin\beta) \quad \text{Eq. [4]}$$

$$V_{pit} = \int_{-p}^{p} A_{pit}\ (\xi) \cdot d\xi \quad \text{Eq. [5]}$$

Where:

$$r = \sqrt{p^2 - \xi^2} \quad \text{Eq. [6]}$$

$$y = \frac{2R^2 - r^2}{2R} \quad \text{Eq. [7]}$$

$$\alpha = 2 \cdot \cos^{-1}\left(\frac{y}{R}\right) = 2 \cdot \cos^{-1}\left(1 - \frac{r^2}{2R^2}\right) \quad \text{Eq. [8]}$$

$$\alpha = 2 \cdot \cos^{-1}\left(\frac{y}{R}\right) = 2 \cdot \cos^{-1}\left(1 - \frac{r^2}{2R^2}\right) \quad \text{Eq. [9]}$$

With reference to a Φ12 mm bar, it is thus possible to calculate the area and the volume of a progressing pit (from 1 mm up to 12 mm) as in Table 2, from which the time necessary to develop the loss of a specific volume can be estimated (in years). According to (Van Belleghem, 2018), a loss of 13.36 mm^3 was estimated for a period of 20 weeks, and 0.58 mm^3 per week from 20 weeks onwards. These results are obtained from an experimental campaign based on a fly ash containing concrete, with a water-to-binder (W/B) ratio of 0.41 and a fly ash-to-binder (FA/B) ratio of 15%. This mixture was designed to be a representative reference mixture for concrete in exposure class XS2, i.e. submerged reinforced concrete subject to corrosion initiated by chlorides. The specimens, with an approximate crack width of 300 µm, were exposed to a 33 g/L NaCl solution in order to simulate a chloride containing environment (sea water, typically) and adopting two exposure regimes. One of these consisted of a 3.5 day wet period followed by a 3.5 day dry period, for 26 weeks in total, while the second one was changed to a 1 day wet period followed by a 6 day dry period for a total of 44 weeks (Van Belleghem, 2018).

3.2 Crack filling by means of resin

Since cracks affect the overall durability of a concrete structure, a repair solution could be to fill them with chemical resins (epoxy, acrylic and polyurethane) acting as an offset and stopping the ingress of the external agents (SIKA, 2015). ACI 503R report identifies the resin injection as an efficient method for crack repair in buildings, bridges, dams and other types of concrete structures (ACI, 1998) while several guidelines and methods of application are described in ACI 504R (ACI, 1997). Furthermore, thanks to their mechanical properties, the resins can be able to restore the structure stiffness (Araújo, 2016)(Schmid, 2010) and, moreover, the polyurethane, expanding during the injection, guarantees strong adhesion to the concrete both in wet and dry cracks, ensuring the regain in impermeability. Therefore, one of the repairing techniques that this study analyzes, is the filling of the cracks by means of a pressure-injected polyurethane resin, since it is a commonly used method in Belgium and several countries worldwide. More specifically it was supposed to employ a commercial one-component polyurethane-based resin. As the technical specifications clarify, these kind of products are recommended to be injected at a pressure of 14 bar up to 200 bar. The product is pumped into the cracks by holes drilled at an angle of 45° distributed around the crack at a distance that, according to the specific situation, can vary from 150 mm up to 900 mm. A schematic representation of the procedure is reported in **Figure 6**. Furthermore, according to what is stated in (Tilly and Jacobs, 2007) in which the concrete repair performances throughout the service life are assessed, it was assumed that around 90% of the cracks filling will fail in 25 years requiring further injections to restore the integrity of the structure.

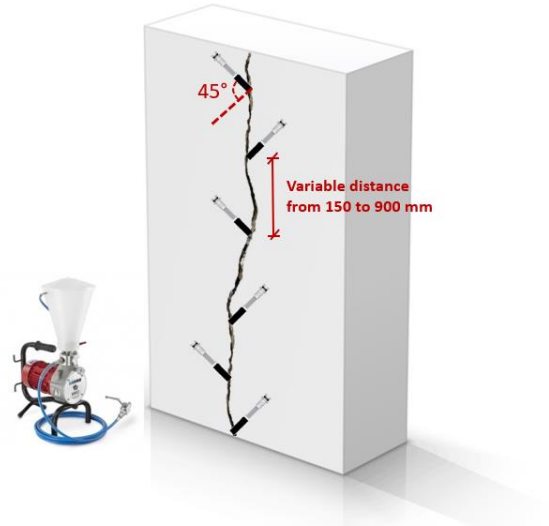

***Figure 6**: Schematic representation of polyurethane resin injection*

4 Life cycle assessment

The LCA, according to ISO 14040-14044 (UNI, 2021a)(UNI, 2021b), consists of four steps: 1) definition of the goal and scope, 2) inventory analysis, 3) impact analysis and 4) interpretation.

4.1 Definition of the goal and scope

This study aims at quantifying the environmental and cost benefits of the SAP-based concrete solution in comparison to the traditional one. To this purpose, the authors have used a cradle-to-gate system boundary being aware that the best practice should include the “end-of-life” scenario extending the cradle-to-gate to a cradle-to-grave system boundary at least. However, considering that the analyzed

composites are still under development and being aware of the lack of information regarding the disposal scenario or the recyclability option which is still under development (Snoeck et al., 2021), it is not possible to include the end-of-life phase. In fact, the presence of SAPs could imply a specific disposal specification for the entire structure, that is still unknown at the time of writing. Therefore, the goal of highlighting the possible environmental benefits of these innovative materials, is pursued taking into account the impacts referring to the production and use stages that correspond to the A1-B7 stages indicated in EN 15804 (UNI, 2019) as reported in **Table 3**.

***Table 3**: Life cycle stages for construction products – EN15804*

PRODUCTION			CONSTRUCTION		USE							END OF LIFE				BENEFITS
A1	A2	A3	A4	A5	B1	B2	B3	B4	B5	B6	B7	C1	C2	C3	C4	D
Raw materials supply	Transport	Manufacturing	Transport	Construction	Use	Maintenance	Repair	Replace	Refurbishment	Operation energy use	Operational water use	Demolition	Transport	Waste processing	Disposal	Reuse/Recovery/recycling potential

For the purpose of this research a Functional Unit (FU) corresponding to the wall itself was selected with a service life varying from 50 years up to 100 years according to four different scenarios. With regard to the reference structure, since several vertical cracks were already observed after 5 days; and after 1 month the cracks ranged from 50 up to 110 µm width and varying from 870 mm up to 1,880 mm length (Tenório Filho et al., 2021a) , the two above-mentioned repairing activities were taken into account to restore its functionality. The first technique implies the demolition and the reconstruction of the concrete cover with the substitution of the damaged bars with a pre-treatment of the concrete cover substrate prior to the casting of the new layer. When the uniform corrosion propagation rate is taken into account, the associated impacts and costs are below indicated with Wall_Ref_M1_50 and Wall_Ref_M1_100 referring to 50 and 100 years of SL according to the specific scenario. When the hemispherical pit model is taken into account, then the associated environmental burdens and overall costs are indicated with Wall_Ref_M2_50 and Wall_Ref_M2_100 for 50 and 100 years of SL respectively. The second refurbishment option for the reference structure, consists of the injection by pressure of a polyurethane resin into the cracks, assuming that, as stated in 3.2, after 25 years it is necessary to reiterate the activity for 90% of the cracks already filled in the past. The impacts associated to this second option are described in what is below indicated with Wall_Resin 50 and Wall_Resin 100 depending on the considered timeframe. With regard to the SAPs-based structure, it is supposed to be subjected to the same corrosion propagation models as the reference wall, but, since no cracks were observed up to 9 months, just the concrete cover reconstruction with the replacement of the damaged bars are taken into account. This, according to what was stated before, allows to restore the M_{Rd} values to the original ones obtaining an extension in terms of service life as shown by way of example in **Fig. 7** for the case of Wall_SAP.

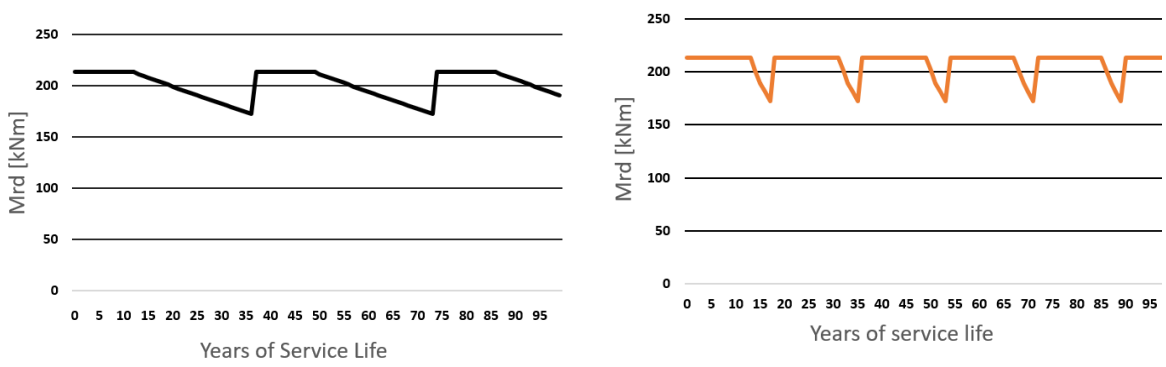

***Figure 7**:* Representation of M_{Rd} as a function of time and its "upgrade" along the service life thanks to the retrofitting operations adopting the corrosion rate from the literature (on the left) and the hemispherical pit model (on the right) for the case of Wall_SAP. The increases in M_{Rd} correspond to the time when the repairing activities are carried out.

4.2 Life cycle inventories (LCI)

4.2.1 Data source

Ecoinvent 3.6 was used as data source for collecting the LCIs for all raw materials both for traditional and SAP-containing concrete. This was not difficult for most of the common constituents like sand/gravel/cement/water, but needed further and dedicated investigation for data referring to commercial products such as SAPs, epoxy resin and superplasticizers. About the latter, the existing libraries contain data only for plasticizers based on sulfonated melamine formaldehyde while in the concrete matrix a polycarboxylate-based one, was also used. Therefore, a modelled version by Agustí-Juan et al. (Agustí-Juan et al., 2017) was used and reported in Table 4 in accordance to the Environmental Product Declaration (EPD) of the product (European Federation of Concrete admixtures Associations Ltd, 2019).

***Table 4**: LCI used for the polycarboxylate-based plasticizer*

Materials/fuels	Amount	Unit
Chemical, organic (GLO)| market for | APOS,U	0.167	kg
Formaldehyde (GLO) | market for | APOS,U	0.038	kg
Sodium hydroxide, without water, in 50% solution state (GLO) | market for | APOS,U	0.137	kg
Sulfuric acid (GLO) | market for | APOS,U	0.162	kg
Water, completely softened, from decarbonised water, at user (GLO)| market for | APOS,U	0.496	kg

The SAP was modeled as a commercially available synthetic polymer, made of acrylamide and sodium acrylate (Table 5). As the exact composition is confidential, some assumptions, based on the existing literature, had to be made to model its LCI. The employed SAP was considered as a 30% anionic synthetic polymer, made of acrylamide and sodium acrylate. This implies that 30 mol% of the monomers incorporated in the SAP are negatively charged while the remaining ones are divided into 60 mol% acrylamide and 10 mol% crosslinker (that, for the polymerization purpose, could be

methylene bisacrylamide). Then, using 71.08 g/mol, 94.04 g/mol and 154.17 g/mol as molar masses for acrylamide, sodium acylate and crosslinker respectively, the mol-% were calculated into mass-%.

***Table 5** : SAP_acrylamide / sodium acrylate LCI*

Known outputs to technosphere	**Amount**	**Unit**
SAP_ acrylamide / sodium acrylate	1	kg
Known inputs from technosphere	**Amount**	**Unit**
Polyacrylamide {GLO}|market for|APOS,U	0.326	kg
Acrylate	0.494	kg
Ammonium persulfate (as modeled after Gontia & Janssen)	0.004	kg
Polyacrylamide {GLO}|market for|APOS,U (adopted as crosslinker)	0.178	kg
Water, deionised, from tap water, at user {GLO}| market for | Alloc Def, U	2	kg
Electricity, medium voltage {BE}|market for|APOS,U *(for stirring)*	0.001	kWh
Electricity, medium voltage {BE}|market for|APOS,U *(for flushing)*	0.094	kWh
Electricity, medium voltage {BE}|market for|APOS,U *(for drying)*	4.138	kWh
Electricity, medium voltage {BE}|market for|APOS,U *(for grinding)*	0.016	kWh

Furthermore, as can be observed in Table 5, due to the lack of data regarding the methylene bisacrylamide as crosslinker, polyacrylamide (the most similar one from a chemical point of view) was used for the specific purpose. This assumption is based on the fact that polyacrylamide is a polymer resulting from acrylamide polymerization while methylene bisacrylamide is chemically similar to the acrylamide monomer. Additionally, 2 kg of water were assumed as necessary during the polymerization phase while for the energy consumptions values the ones stated by Van Den Heede et al., for the synthetic acrylic acid + acrylamide based SAP, have been adopted (Van den Heede et al., 2018). Here, the ones referred to the heating process, typically required to initiate the polymerization in case a thermal photo-initiator is used, were excluded since this was not the case. With reference to the concrete manufacturing, as already done by Van den Heede et al., also the impacts referring to the production process at a ready-mix concrete plant have been incorporated. The existing Ecoinvent LCI for concrete mixing (*Concrete, normal {CH}| unreinforced concrete production, with cement CEM II/A | APOS, U*') was used after a slight modification. In fact, removing 'Gravel, round {CH}| market for gravel, round | APOS, U', 'Cement, alternative constituents 6-20% {CH}| market for | APOS, U' and 'Tap water {CH}| market for | APOS, U' from the existing LCI, it was possible to obtain the specific inventory referring to the act of concrete mixing on an industrial scale. No inventory data were readily available in Ecoinvent 3.6 for the acrylate; for this reason, as shown in Table 6, the LCI adopted by Gontia and Janssen (Gontia and Janssen, 2016) for the sodium poly(acrylate), excluding the ammonium persulfate and sodium hydroxide, was used. The former is the initiator for the polymerization and does not play a role in the production of the acrylate monomer as such. With regard to consumption of electricity, the same value was assumed as for acrylamide, due to the fact that the production process requires approximately the same amount of energy.

Table 6: Acrylate LCI

Known outputs to technosphere	**Amount**	**Unit**
Acrylate	1	kg
Known inputs from technosphere	**Amount**	**Unit**
Acrylic acid {GLO}| market for | APOS,U	0.782	kg
Electricity, medium voltage {BE}| market for | APOS,U	7.830	MJ
Water, deionised, from tap water, at user {GLO}| market for | APOS,U	1.753	kg
Emissions to water	**Amount**	**Unit**
Water	1.953	kg

About the polyurethane resin injection, the EPD (FEICA - Association of the European Adhesive and Sealant Industry, 2015a) of a commercial product, already provides the CML_IA impacts values referred to the production process. These impacts, scaled on the basis of the quantity of the included product, were simply added to the ones referring to Wall_Resin construction itself. Anyway, since they were not exhaustive enough, it was necessary to estimate the impact of the whole injection process too. To do this, the use of a rotary hammer with a 850 W of power to drill the holes and an equipment for the injection by pressure with 750 W power to pump the product were considered. As the time needed to complete the process can vary according to the boundary conditions, a time of around 1 hour to drill all the holes and of 8 hours to fill the cracks was roughly estimated. Therefore 0,972 kWh and 6 kWh of the Ecoinvent data “Electricity, medium voltage {BE}| market for | Alloc Def, U” have been respectively used to estimate the act of drilling and the resin injection. Regarding the replacement of the damaged reinforcement bars with the concrete cover substitution, the concrete substrate is usually treated with specific epoxy adhesives to ensure a good adhesion of the new cover. For this scope, a commercial product was considered of which the associated impacts, starting from the preparation of a perfectly clean and solid substrate until its on-site installation, were deduced from its EPD (FEICA - Association of the European Adhesive and Sealant Industry, 2015b) and scaled on the basis of the quantity of the necessary product and added to the ones referring to Wall_Ref. As possible to observe in this paragraph and in Table 4, Table 5 and Table 6, for all the data taken from the Ecoinvent library, the model named Allocation at the Point Of Substitution (APOS) has been chosen. This in order to valorize the potential recycling and the reuse possibilities of a product due to the partial allocation of impacts.

4.3 Impact analysis

The environmental footprint of the FU has been calculated using the CML-IA impact method, representing an update of the CML 2 baseline 2000 method, which was released by the Center of Environmental Science (CML) of Leiden University in 2013. It gives a general overview of 10 impact indicators in total: global warming (GWP); acidification (AP); ozone depletion (ODP); photochemical oxidation (POCP); eutrophication (EP); abiotic depletion potential (ADP); human toxicity potential (HTP); freshwater aquatic ecotoxicity potential (FAETP); marine aquatic ecotoxicity (MAETP) and terrestrial ecotoxicity potential (TETP). The entire analysis was developed using the software SimaPro.

4.4 Impacts calculation and interpretation

The different conditions in which the FU is assessed are below better described and discussed. Furthermore, in each scenario, which only takes into account the concrete cover reconstruction and the replacement of the damaged steel bars, the related environmental impacts are compared to the

impacts of the scenarios with the epoxy resin injection. The latter scenarios include more specifically Wall_Resin_50 and Wall_Resin_100 depending on the considered timeframe of 50 years or 100 years respectively. With regard to the frequency of the resin injections, according to section 3.2, two reiterations were taken into account for Wall_Resin_50 while 4 were considered for Wall_Resin_100. The frequency of the maintenance activities are estimated as better detailed in sections 4.4.1 to 4.4.4 and summarized in Table 7.

4.4.1 Scenario 1

The first scenario is limited to 50 years of service life. As described in 3.1.1, the structural stability is compromised when the tension bars lose 89% of their cross-section but it is reasonably considered that the maintenance works are carried out already when the bar loses 20% of its cross-section. This is in line with what is considered in studies like the one by Zhang et al.(Zhang et al., 2021) in which it is outlined that when the corrosion loss exceeds 15% it causes a critical concrete damage able to affect shear behavior of reinforced concrete beams. Also in (Noh et al., 2018), assessing the case of a beam of which the reinforcement is subjected to different corrosion scenarios, it is stated that 20% degree of corrosion causes significant reduction in terms of strength capacity. In this scenario, to calculate the frequency of these activities, the corrosion rate described in 3.1.4 and Fig. 4 was used. For the case of the reference solution, in this scenario identified as Wall_Ref_M1_50, the first repairing activities are estimated to be developed after 25 years, including the initiation period which is almost equal to 0 for the case of cracked concrete. Then, since the new concrete cover is supposed to be un-cracked, an initiation period of 13 years was added to the remaining time to lose 20% of the cross section (again, 25 years). With regard to the SAPs-based structure, for this case indicated as Wall_SAP_M1_50, a calculated period of 13 years and 25 years were used for the initiation and propagation respectively. According to this, for scenario 1, only one repairing activity is taken into consideration for both Wall_Ref_M1_50 and Wall_SAP_M1_50..

4.4.2 Scenario 2

The second scenario considers the same corrosion rate as before but extending the service life up to 100 years. The initiation and propagation times are the same as for Scenario 1 with a resulting reiteration for the maintenance activity of 3 and 2 times for the reference structure and the SAPs based one, represented by Wall_Ref_M1_100 and Wall_SAP_M1_100 respectively.

4.4.3 Scenario 3

In the third scenario, the selected FU is analyzed in a timeframe of 50 years but using the corrosion model described in 3.1.5. As above, considering the necessity to carry out maintenance activities when the steel bars lose 20% of their cross-section, a corrosion pit equal to 4 mm according to the values reported in **Table 2** was taken into account. Therefore, considering that the initiation periods will remain the same as for Scenario 1 and 2, assuming a propagation time equal to 3.8 years, in this scenario are taken into consideration 3 and 2 maintenance activities for the reference and the SAPs-based solution respectively, here indicated as Wall_Ref_M2_50 and Wall_SAP_M2_50 respectively.

4.4.4 Scenario 4

The final scenario adopts the same hemispherical pit model as before within a service life of 100 years. This framework allows to better highlight the enhanced eco-performances of the SAP technology in comparison to conventional solution. Here, according to what was stated above, seven and five maintenance activities are taken into account for Wall_Ref_M2_100 and Wall_SAP_M2_100 respectively.

519 ***Table 7***: Summary of the maintenance activities

	Nr. of epoxy resin injections	Adopted corrosion model	Initiation time	Propagation time	Nr. of concrete cover reconstruction and rebars substitution
Wall_Resin 50	**2**	-	-	-	-
Wall_Resin 100	**4**	-	-	-	-
Wall_Ref_M1_50	-	50 µm/year	0 (if cracked) or 13 years (if uncracked)	25 years	**1**
Wall_Ref_M1_100	-	50 µm/year	As above	25 years	**3**
Wall_Ref_M2_50	-	Hemispherical pit model	As Above	3.8 years	**3**
Wall_Ref_M2_100	-	Hemispherical pit model	As above	3.8 years	**7**
Wall_SAP_M1_50	-	50 µm/year	13 years	25 years	**1**
Wall_SAP_M1_100	-	50 µm/year	As above	25 years	**2**
Wall_SAP_M2_50	-	Hemispherical pit model	As Above	3.8 years	**2**
Wall_SAP_M2_100	-	Hemispherical pit model	As above	3.8 years	**5**

520 ## 4.5 LIFE CYCLE COST

521

522 The European Community, already in 2008, defined the concept of Green Public Procurement (GPP) as
523 a voluntary instrument used by the authorities to procure goods, services and works with reduced
524 environmental impacts. Its use should lead the industry to develop green technologies and products.
525 In this framework, the importance of the cost assessment is based on a product life-cycle. In relation
526 to the civil sector this means that the construction price just represents one element of the entire
527 estimation, since also the hidden costs related to the maintenance activities can be relevant.
528 Therefore, the Life Cycle Cost (LCC) was here used to better state the potential of the investigated
529 advanced concrete materials determining the potential cost-effectiveness throughout the entire
530 service life. Since much information was lacking, part of this work consisted of a market survey to
531 collect the necessary data. In fact, except for the cost of SAPs, already outlined by Snoeck (Snoeck,
532 2015), "casting of concrete C 35/45", "casting of concrete C30/37" and "supply and installation of
533 rebars" rates were obtained from company perspectives. For the remaining ones, as no further bill of
534 quantities (BoQ) were found for the Belgium construction market, after verifying that the above-
535 mentioned rates were comparable to the Italian ones, they were obtained from the Italian construction
536 costs list (Provveditorato interregionale per la Lombardia e l'Emilia Romagna, 2021). Additionally, since
537 the maintenance activities will be developed in the future, it has been necessary to adopt the principle
538 suggested by EN 16627:2015 (UNI, 2015) to calculate the value today for an economic transaction in
539 the future by using a discount factor as the following equation indicates:

540 $$\boldsymbol{CF(T)=1/(1+r)^{T}} \quad \text{Eq. [10]}$$

where r is the annual real discount rate and T is the number of future years. The annual real discount rate, which has to be determined through a sensitivity analysis on at least two different rates, one of which shall be 3% expressed in real terms according to the EN 16627:2015 (UNI, 2015) and to the Commission Delegated Regulation n°244/2012 of 16 January 2012 (Commission Delegated Regulation, 2012), is then assumed equal to 3% according to (Caruso et. Al, 2020). Therefore, all the rates referred to maintenance activities to be developed in the future have been actualized according to Eq. 10, assuming a variable T value, up to 100 years.

***Table 8**: Wall_REF construction costs. Note: here refurbishment works are not included*

Wall_Ref

Work	**Rate per unit (€)**	**quantity**	**unit**	**Amount (€)**
Casting of concrete C 35/45	78.70	30.08	m^3	2,367.29
Supply and installation of rebars	0.95	1,933	kg	1,836.35
Formworks up to 4 m of height	35.95	77	m^2	2,768.15
			sum	6,971.80
unexpected costs (10%)				697.18
TOTAL				**7,669.00**

***Table 9**: Wall_SAP construction costs. Note: here refurbishment works are not included*

Wall_SAP

Work	**Rate per unit (€)**	**quantity**	**unit**	**Amount (€)**
Casting of concrete C 30/37	75.00	30.08	m^3	2,256.00
Supply and installation of rebars	0.95	1,800	kg	1,710.00
Formworks up to 4 m of height	35.95	77.00	m^2	2,768.15
Commercial SAP	10.00	40.9	kg	409.00
			sum	7,143.15
unexpected costs (10%)				714.32
TOTAL				**7,857.00**

***Table 10**:* Wall_Resin 50 construction costs. Rates marked with "*" are calculated according to the discount factor depending on when the maintenance activity will be carried out.

Wall_Resin 50

Work	**Rate per unit (€)**	**quantity**	**unit**	**Amount (€)**
Casting of concrete C 35/45	78.70	30.08	m^3	2,367.30
Supply and installation of rebars	0.95	1,933	kg	1,836.35
Formworks up to 4 m of height	35.95	77	m^2	2,768.15
Polyurethane resin injection by pressure	240.00	11.03	m	2,647.20
Extra polyurethane resin injection by pressure*	variable*	9.97	m	1,1142.81
			sum	10,761.81
unexpected costs (10%)				1,076.18

TOTAL				**11,838.00**

556

557 ***Table 11***: Wall_Resin 100 construction costs. Rates marked with "*" are calculated according to the discount factor
558 depending on when the maintenance activity will be carried out.

Wall_Resin 100

Work	**Rate per unit (€)**	**quantity**	**unit**	**Amount (€)**
Casting of concrete C 35/45	78.70	30.08	m^3	2,367.30
Supply and installation of rebars	0.95	1,933	kg	1,836.35
Formworks up to 4 m of height	35.95	77	m^2	2,768.15
Polyurethane resin injection by pressure	240.00	11.03	m	2,647.20
Extra polyurethane resin injection by pressure	variable*	28.91	m	1,949.31
			sum	11,568.31
unexpected costs (10%)				1,156.31
TOTAL				**12,725.00**

559

560 ***Table 12***: Wall_SAP with concrete cover reconstruction and steel rebars substitution, Scenario 1. Rates marked with "*" are
561 calculated according to the discount factor depending on when the maintenance activity will be carried out.

Wall_SAP_M1_50

Work	**Rate per unit (€)**	**quantity**	**unit**	**Amount (€)**
Casting of concrete C 30/37	75.00	30.08	m^3	2,256.00
Supply and installation of rebars	0.95	1,800	kg	1,710.00
Formworks	35.95	77.00	m^2	2,768.15
Commercial SAP	10.00	40.9	kg	409.00
Extra commercial SAP	variable*	1.56 in total	kg	5.07
Extra Formworks*	variable*	38.5 in total	m^2	450.14
Demolition of damaged concrete*	variable*	1.15 in total	m^3	28.05
Transport of waste material to landfill*	variable*	1.15 in total	m^3	17.80
Extra concrete casting*	variable*	1.15 in total	m^3	28.05
			sum	7,672.26
unexpected costs (10%)				767.23
TOTAL				**8,439.00**

562

563 ***Table 13***: Wall_SAP with concrete cover reconstruction and steel rebars substitution, Scenario 2. Rates marked with "*" are
564 calculated according to the discount factor depending on when the maintenance activity will be carried out.

Wall_SAP_M1_100

Work	**Rate per unit (€)**	**quantity**	**unit**	**Amount (€)**
Casting of concrete C 30/37	75.00	30.08	m^3	2,256.00
Supply and installation of rebars	0.95	1,800	kg	1,710.00
Formworks	35.95	77.00	m^2	2,768.15
Commercial SAP	10.00	40.9	kg	409.00

Extra commercial SAP	variable*	3.12 in total	kg	6.72
Extra Formworks*	variable*	77 in total	m^2	596.53
Demolition of damaged concrete*	variable*	2.30 in total	m^3	37.17
Transport of waste material to landfill*	variable*	2.30 in total	m^3	23.59
Extra concrete casting*	variable*	2.30 in total	m^3	37.17
			sum	7,844.34
unexpected costs (10%)				784.43
TOTAL				**8,629.00**

565

566 ***Table 14****:* Wall_SAP with concrete cover reconstruction and steel rebars substitution, Scenario 3. Rates marked with "*" are
567 calculated according to the discount factor depending on when the maintenance activity will be carried out

Wall_SAP_M2_50

Work	**Rate per unit (€)**	**quantity**	**unit**	**Amount (€)**
Casting of concrete C 30/37	75.00	30.08	m^3	2,256.00
Supply and installation of rebars	0.95	1,800	kg	1,710.00
Formworks	35.95	77.00	m^2	2,768.15
Commercial SAP	10.00	40.9	kg	409.00
Extra commercial SAP	variable*	3.12 in total	kg	6.72
Extra Formworks*	variable*	77 in total	m^2	1,355.01
Demolition of damaged concrete*	variable*	2.30 in total	m^3	84.43
Transport of waste material to landfill*	variable*	2.30 in total	m^3	53.57
Extra concrete casting*	variable*	2.30 in total	m^3	84.43
			sum	8,735.89
unexpected costs (10%)				873.59
TOTAL				**9,609.00**

568

569 ***Table 15****:* Wall_SAP with concrete cover reconstruction and steel rebars substitution, Scenario 4. Rates marked with "*" are
570 calculated according to the discount factor depending on when the maintenance activity will be carried out.

Wall_SAP_M2_100

Work	**Rate per unit (€)**	**quantity**	**unit**	**Amount (€)**
Casting of concrete C 30/37	75.00	30.08	m^3	2,256.00
Supply and installation of rebars	0.95	1,800	kg	1,710.00
Formworks	35.95	77.00	m^2	2,768.15
Commercial SAP	10.00	40.9	kg	409.00
Extra commercial SAP	variable*	10.92 in total	kg	22.21
Extra Formworks*	variable*	269.50 in total	m^2	1,972.47
Demolition of damaged concrete*	variable*	8.05 in total	m^3	122.92
Transport of waste material to landfill*	variable*	8.05 in total	m^3	77.99
Extra concrete casting*	variable*	8.05 in total	m^3	122.92
			sum	9,461,66
unexpected costs (10%)				946.17
TOTAL				**10,408.00**

571

572 ***Table 16****:* Wall_ref with concrete cover reconstruction and steel rebars substitution, Scenario 1. Rates marked with "*" are
573 calculated according to the discount factor depending on when the maintenance activity will be carried out.

Wall_Ref_M1_50

Work	**Rate per unit (€)**	**quantity**	**unit**	**Amount (€)**
Casting of concrete C 35/45	78.70	30.08	m^3	2,367.29
Supply and installation of rebars	0.95	1,933	kg	1,836.35
Extra rebars supply and installation*	variable*	244.2 in total	kg	110.80
Formworks	35.95	77	m^2	2,768.15
Extra Formworks*	variable*	38.5 in total	m^2	661,04
Demolition of damaged concrete*	variable*	1.15 in total	m^3	43,41
Transport of waste material to landfill*	variable*	1.15 in total	m^3	26.25
Extra concrete casting*	variable*	1.15 in total	m^3	43.41
			sum	7,856.72
unexpected costs (10%)				785,67
TOTAL				**8,642.00**

574

575 ***Table 17****:* Wall_Ref with concrete cover reconstruction and steel rebars substitution, Scenario 2. Rates marked with "*" are
576 calculated according to the discount factor depending on when the maintenance activity will be carried out.

Wall_Ref_M1_100

Work	**Rate per unit (€)**	**quantity**	**unit**	**Amount (€)**
Casting of concrete C 35/45	78.70	30.08	m^3	2,367.29
Supply and installation of rebars	0.95	1,933	kg	1,836.35
Extra rebars supply and installation*	variable*	732.6 in total	kg	158.55
Formworks	35.95	77	m^2	2,768.15
Extra Formworks*	variable*	115.5 in total	m^2	945.95
Demolition of damaged concrete*	variable*	3.45 in total	m^3	61.68
Transport of waste material to landfill*	variable*	3.45 in total	m^3	37.40
Extra concrete casting*	Variable*	3.45 in total	m^3	61.68
			sum	8,237.42
unexpected costs (10%)				823.74
TOTAL				**9,061.00**

***Table 18**:* Wall_Ref with concrete cover reconstruction and steel rebars substitution, Scenario 3. Rates marked with "*" are calculated according to the discount factor depending on when the maintenance activity will be carried out.

Wall_Ref_M2_50

Work	**Rate per unit (€)**	**quantity**	**unit**	**Amount (€)**
Casting of concrete C 35/45	78.70	30.08	m^3	2,367.29
Supply and installation of rebars	0.95	1,933	kg	1,836.35
Extra rebars supply and installation*	variable*	732.6 in total		410.33
Formworks	35.95	77	m^2	2,768.15
Extra Formworks*	variable*	115.5 in total	m^2	2,448.07
Demolition of damaged concrete*	variable*	3.45 in total	m^3	160.08
Transport of waste material to landfill*	variable*	3.45 in total	m^3	96.80
Extra concrete casting*	variable*	3.45 in total	m^3	160.08
			sum	10,247.16
unexpected costs (10%)				1,024.72
TOTAL				**11,272.00**

***Table 59**:* Wall_Ref with concrete cover reconstruction and steel rebars substitution, Scenario 4. Rates marked with "*" are calculated according to the discount factor depending on when the maintenance activity will be carried out.

Wall_Ref_M2_100

Work	**Rate per unit (€)**	**quantity**	**unit**	**Amount (€)**
Casting of concrete C 35/45	78.70	30.08	m^3	2,367.29
Supply and installation of rebars	0.95	1,933	kg	1,836.35
Extra rebars supply and installation*	variable*	1,465.2 in total	kg	502.83
Formworks	35.95	77	m^2	2,768.15
Extra Formworks*	variable*	192.5 in total	m^2	2,999.93
Demolition of damaged concrete*	variable*	5.75 in total	m^3	196.17
Transport of waste material to landfill*	variable*	5.75 in total	m^3	118.62
Extra concrete casting*	variable*	5.75 in total	m^3	196.17
			sum	10,985.51
unexpected costs (10%)				1,098.55
TOTAL				**12,084.00**

5 Results and discussion

The 4 different scenarios detailed in sections 4.4.1, 4.4.2, 4.4.3 and 4.4.3 lead to obtain different results in terms of environmental and cost impacts. With regard to scenario 1, as shown in **Fig. 8** the impacts

reduction between Wall_SAP_M1_50 and Wall_Ref_M1_50 is generally limited and lower than 5% while the one between Wall_Resin 50 and Wall_Ref_M1_50 is more pronounced reaching 9% for the case of Photochemical oxidation. Additionally, except for the case of GWP, ODP and ADP, under scenario 1, the reinforcement content always causes higher impacts in comparison to the cement ones. Differently to what has been highlighted in Scenario 1, as shown in **Fig. 8**, Scenario 2 better highlights the environmental advantages of Wall_SAP_M1_100 in comparison to Wall_Ref_M1_100, reaching reductions higher than 10% for the case of HTP, FAETP, TETP and POCP while Wall_Resin 100 in comparison to Wall_Ref_M1_100 registers differences always higher than 15% except for EP. This is mainly due to the reiteration of the maintenance activities to be developed throughout the entire service life here extended up to 100 years. Also in this case, the reinforcement amount affects stronger the final results for most of the impact indicators in comparison to the cement content. What was observed with regard to the impacts associated to the cement and reinforcement content under scenario 1 is also confirmed in scenario 2. Moreover, with regard to Scenario 3, **Fig. 8** shows that since for Wall_Ref_M2_50 and Wall_SAP_M2_50 the number of the maintenance activities are the same as for Wall_Ref_M1_100 and Wall_SAP_M1_100, no relevant differences can be remarked in comparison to Scenario 2. Additionally, it must be noted that the effect of the epoxy resin for all the ten impact indicators is almost neglectable with no relevant differences between Wall_Resin_50 and Wall_Resin_100. Thus, comparing Wall_Resin_50 to Wall_Ref_M2_50, the considerations are the same as for scenario 2 between Wall_Resin_100 and Wall_Ref_M1_100. The highest reduction values are reached for the case of Scenario 4 as shown in Fig. 8 having considered a SL of 100 years together with the more aggressive corrosion model such as the hemispherical pit one. For this case, the highest reductions are achieved for FAETP (20%) with values higher than 15% also for MAETP, TETP, POCP and AP. Furthermore, comparing Wall_Resin_100 to Wall_Ref_M2_100, the reductions are always higher than 15% with values around 67% as in the case of HTP. With regard to the costs, despite the addition of the SAP, whose cost is assessed at around 10 € per kg, due to the reduced amount of reinforcement, the Wall_SAP itself, without any maintenance activity, costs around 7,860 € that is just 2.5% higher as compared to the Wall_REF itself (around 7,670 €) as reported in Table 8 and Table 9. The economic convenience of Wall_SAP in comparison to Wall_Ref is confirmed also taking into account the repairing activities in the four scenarios as detailed in Tables 12 to 19. Significant reductions can be observed in the case of Scenario 3 and 4 where, having considered a more aggressive corrosion model resulting in a more rapid loss of the cross section of the steel bars, it is possible to pass from 11,272.00 € and 12,084.00 € for Wall_Ref_M2_50 and Wall_Ref_M2_100 respectively up to 9,609.00 € and 10,408.00 € for the case of Wall_SAP_M2_50 and Wall_SAP_M2_100 with a reduction of around 14 % in both scenarios. Furthermore, as indicated in Table 10 and Table 11, the maintenance activities by means of polyurethane resin injection bring the total amount up to 11,838.00 € and 12,725.00 € in a timeframe of 50 and 100 years, higher than costs for Wall_SAP assessed in the same timeframe under different boundary conditions. Therefore, as clearly shown in **Figure 9** , the epoxy resin injection represents always the most expensive solution with an incidence of the maintenance activities assessed at around 30 % of the total costs for both Wall_Resin 50 and Wall_Resin 100. The same cost incidence can be observed also for Wall_Ref_M2_50 and Wall_Ref_M2_100 while in the same scenarios Wall_SAP_M2_50 and Wall_SAP_M2_100 maintenance activities generate a lower extra expense of 15% and 22% respectively. **Figure 10** and **Figure 11** show the costs trend in a timeframe of 50 and 100 years respectively, outlining for the FU always a continuous cost increasing from 20 years of service life onwards, except for Wall_SAP in scenario 1 and 2 whose costs increase starting from 30 years of SL.

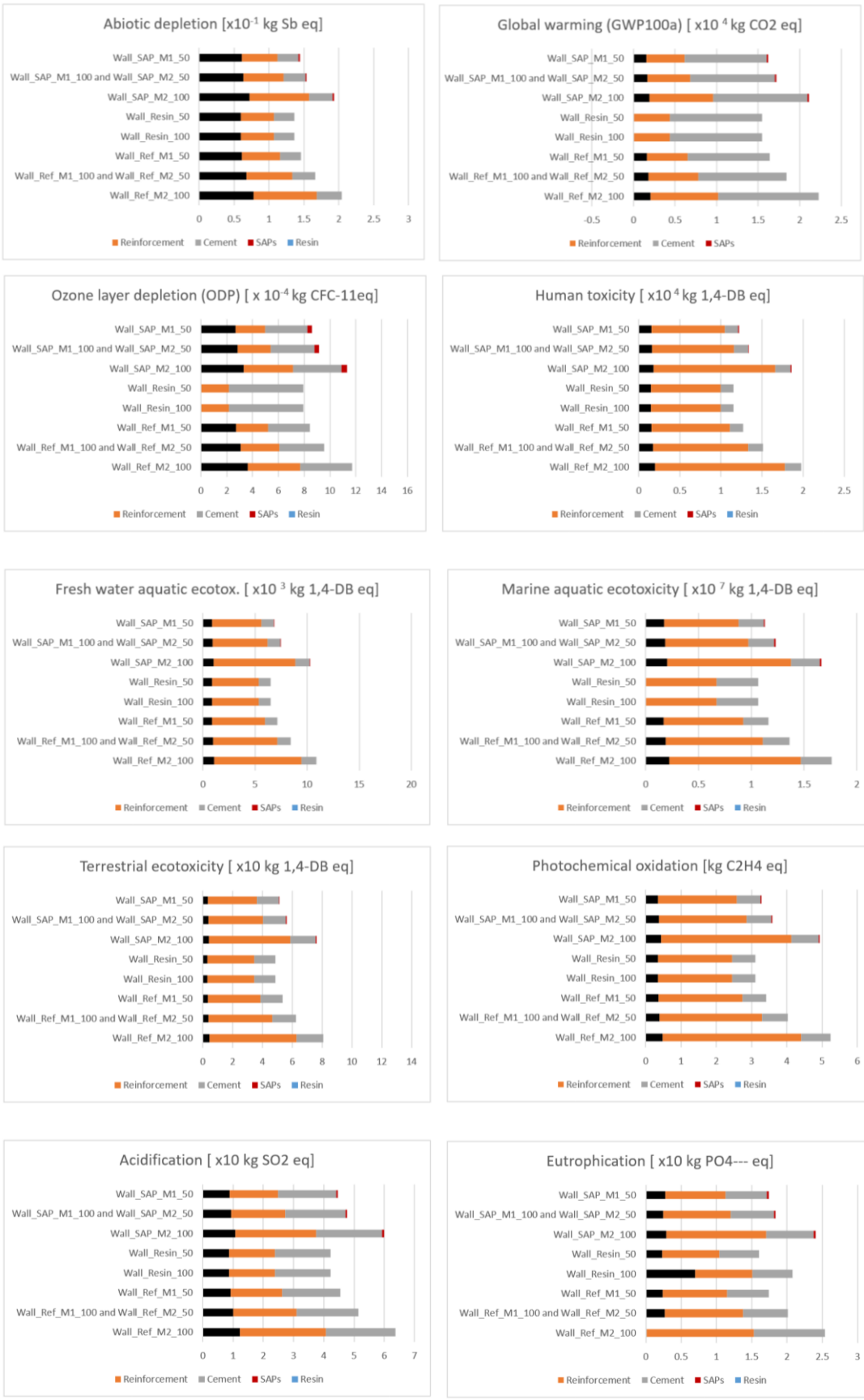

***Figure 8**: Environmental impacts for the different scenarios for the CML impact categories with indication of SAP, cement and reinforcement contribution. The black color represents the environmental burdens due to the remaining components.*

639

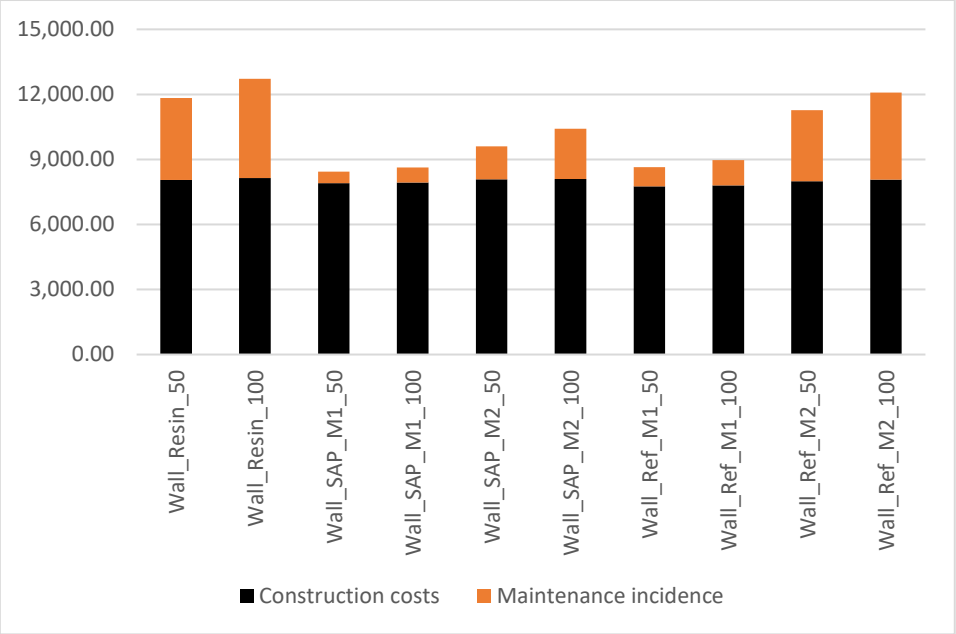

640

641 ***Figure 9:*** Overall costs summary including maintenance incidence (€)

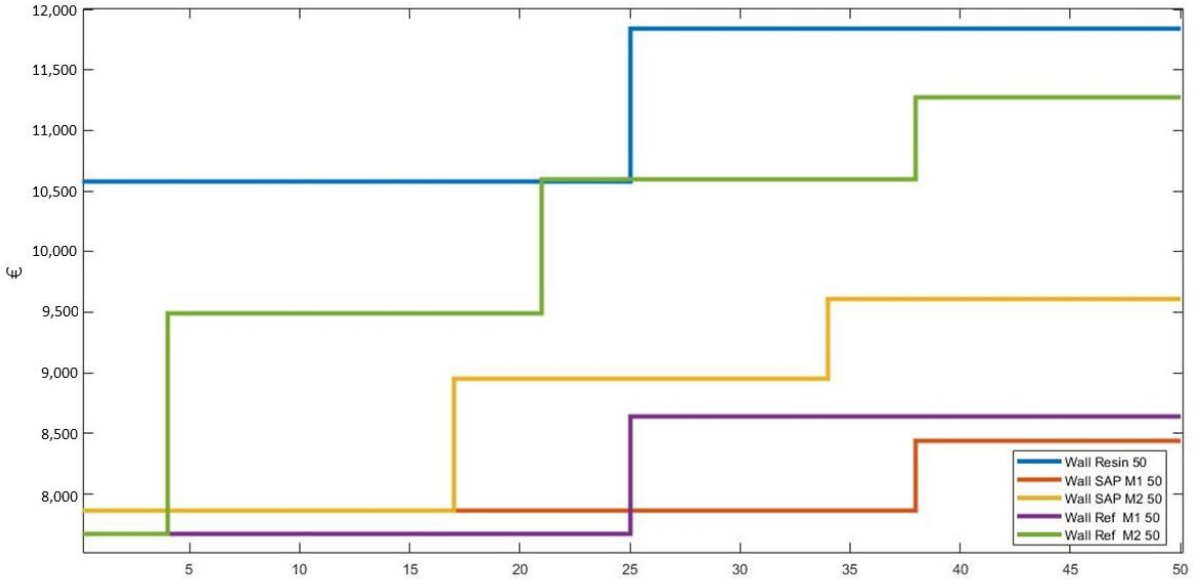

642

Figure 10*: Costs trend within 50 years of service life.*

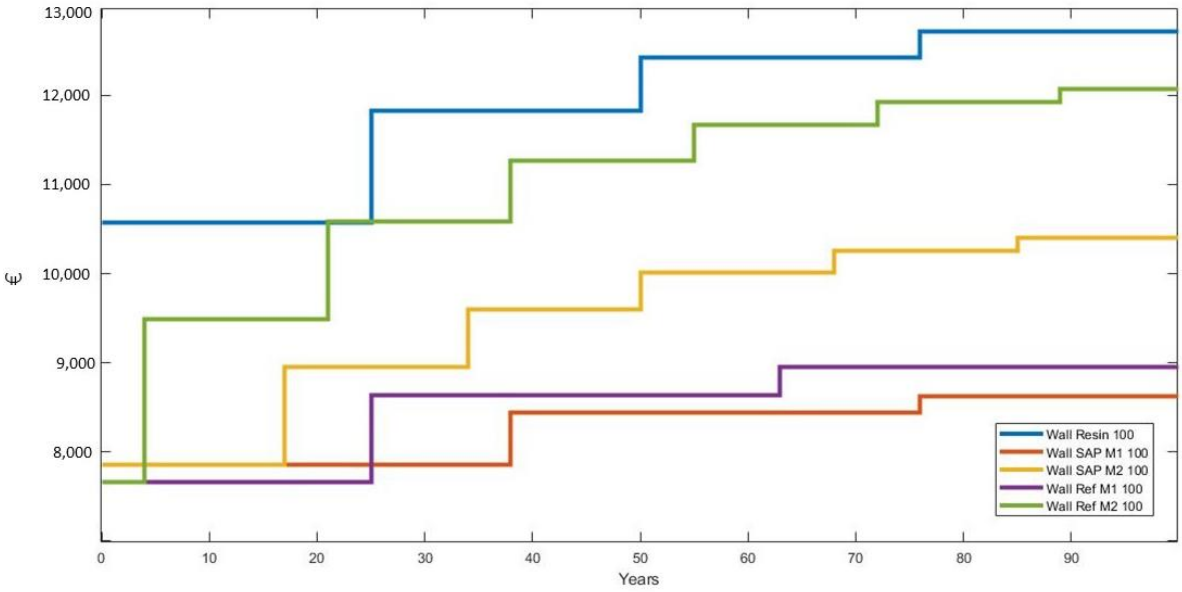

Figure 11: Costs trend within 100 years of service life

6 Conclusions

This paper investigates the use of LCA and LCC methodologies as integral part of the design phase to support the use of SAP-containing concrete in comparison to traditional reinforced concrete solutions. One of the key focus points was to properly estimate the frequency of the repair activities according to the structural properties of the walls and to the durability parameters of a concrete structure exposed to a chloride environment. To this purpose, in this paper, structural design approaches have been combined with equations governing the assessed degradation mechanisms. It is possible to summarize the findings of the research as below:

- it is important, in the material and structural design phase, to target specific durability performance requirements, e.g. in terms of chloride diffusion coefficient values, which govern the corrosion initiation time;
- the maintenance activities are not only responsible for most of the overall costs, summing up to more than 30% in some of the investigated scenarios, but since they imply the use of more reinforcement and cement as well, this inevitably causes higher impacts;
- the influence of the SAPs on the overall impacts is almost neglectable;
- the use of the SAP is the most convenient solution with reference to 50 and 100 years of SL and according to the adopted cradle to gate system boundary;
- the environmental and economic advantages are more significantly evident in longer time frames like 100 years for the case of this study, mainly due to the incidence of the frequency of the maintenance activities.

This highlights the need to act on the durability characteristics and integrate them from the structural design phase. In keeping with this, LCA and LCC are necessary tools to be employed as part of an integrated approach for a more sustainable design of reinforced concrete structures. Such integrated approach will favor the spread and market uptake of innovative solutions in terms of materials and products, like the SAP-containing concrete, which have proven to be promising for the concrete construction industry.

673 # Acknowledgements

This project has received funding from the European Union's Horizon 2020 research and innovation programme under the Marie Skłodowska-Curie grant agreement No 860006.

674 The work within the ICON project iSAP (Innovative SuperAbsorbent Polymers for crack mitigation and
675 increased service life of concrete structures) has been financed by the SIM program SHE (Engineered
676 Self-Healing Materials).
677
678 Philip Van den Heede is a postdoctoral researcher of the Research Foundation - Flanders (FWO)
679 (project No. G062720N). The financial support of FWO is gratefully acknowledged.

680

681 # References

682 ACI 503R-93, Use of Epoxy Compounds with Concrete (Reapproved 1998) American Concrete
683 Institute., n.d.

684 ACI 504R, Guide to Sealing Joints in Concrete Structures (Reapproved 1997) American Concrete
685 Institute., n.d.

686 Agustí-Juan, I., Müller, F., Hack, N., Wangler, T., Habert, G., 2017. Potential benefits of digital
687 fabrication for complex structures: Environmental assessment of a robotically fabricated
688 concrete wall. J. Clean. Prod. 154, 330–340. https://doi.org/10.1016/j.jclepro.2017.04.002

689 Al-Obaidi, S., Bamonte, P., Ferrara, L., Luchini, M., Mazzantini, I., 2020. Durability-based design of
690 structures made with ultra-high-performance/ultra-high-durability concrete in extremely
691 aggressive scenarios: Application to a geothermal water basin case study. Infrastructures 5, 1–
692 44. https://doi.org/10.3390/infrastructures5110102

693 Alonso, M.C., Sanchez, M., 2009. Analysis of the variability of chloride threshold values in the
694 literature. Mater. Corros. 60, 631–637. https://doi.org/10.1002/maco.200905296

695 Araújo, D. de A., 2016. Cracks Repair in Reinforced Concrete Structures Case Study–Reinforced
696 Concrete Tunnel Repair Master dissertation in Civil Engineering.

697 Belleghem, B.V., Van den Heede, P., Tittelboom, K.V., De Belie, N.D., 2017. Quantification of the
698 service life extension and environmental benefit of Chloride Exposed Self-Healing Concrete.
699 Materials (Basel). 10. https://doi.org/10.3390/ma10010005

700 C. Andrade, C. Alonso, J. Rodriguez, et al. Cover cracking and amount of rebar corrosion: importance
701 of the current applied accelerated tests C. Sjostrom (Ed.), Durability of Building Materials and
702 Components, 7, E&FN Spon, London (1996), pp. 263-273, n.d.

703 Caruso, M.C., Pascale, C., Camacho, E., Scalari, S., Animato, F., Alonso, M.C., Gimenez, M., Ferrara, L.,
704 2020. Life cycle assessment on the use of ultra high performance fibre reinforced concretes
705 with enhanced durability for structures in extremely aggressive environments: Case study
706 analyses, RILEM Bookseries. https://doi.org/10.1007/978-3-030-43332-1_24

707 Cen, 2016. UNI EN 206:2016, Concrete - Specification, performance, production and conformity.

708 Cen, 2005a. EN 1992-2:2005, Eurocode 2 - Design of concrete structures - Concrete bridges - Design
709 and detailing rules.

710 Cen, 2005b. EN 1504, Products and systems for the protection and repair of concrete structures -
711 Definitions, requirements, quality control and evaluation of conformity, parts 1-10.

712 Commission Delegated Regulation, 2012. Commission Delegated Regulation (EU), 2012 No 244/2012
713 of 16 January 2012 supplementing Directive 2010/31/EU of the European Parliament and of the
714 Council on the energy performance of buildings by establishing a comparative methodology
715 framework for calculating cost-optimal levels of minimum energy performance requirements
716 for buildings and building elements Text with EEA relevance.

717 Coppola, L., 2007. Concretum. MCGRAW-HILL EDUCATION.

718 Craeye, B., Geirnaert, M., Schutter, G.D., 2011a. Super absorbing polymers as an internal curing
719 agent for mitigation of early-age cracking of high-performance concrete bridge decks. Constr.
720 Build. Mater. 25, 1–13. https://doi.org/10.1016/j.conbuildmat.2010.06.063

721 Craeye, B., Geirnaert, M., Schutter, G.D., 2011b. Super absorbing polymers as an internal curing
722 agent for mitigation of early-age cracking of high-performance concrete bridge decks. Constr.
723 Build. Mater. 25, 1–13. https://doi.org/10.1016/j.conbuildmat.2010.06.063

724 European Federation of Concrete admixtures Associations Ltd. (EFCA)., 2019. ENVIRONMENTAL
725 PRODUCT DECLARATION - Concrete admixtures – Plasticisers and Superplasticisers.

726 Federico, L.M., Chidiac, S.E., 2009. Waste glass as a supplementary cementitious material in concrete
727 - Critical review of treatment methods. Cem. Concr. Compos. 31, 606–610.
728 https://doi.org/10.1016/j.cemconcomp.2009.02.001

729 FEICA - Association of the European Adhesive and Sealant Industry, 2015a. ENVIRONMENTAL
730 PRODUCT DECLARATION - Reactive resins based on polyurethane or SMP, filled or aqueous,
731 solvent-free.

732 FEICA - Association of the European Adhesive and Sealant Industry, 2015b. ENVIRONMENTAL
733 PRODUCT DECLARATION - Reactive resins based on epoxy resin, filled and/or aqueous with low
734 content of filler.

735 Feiteira, J., Gruyaert, E., De Belie, N., 2016. Self-healing of moving cracks in concrete by means of
736 encapsulated polymer precursors. Constr. Build. Mater. 102, 671–678.
737 https://doi.org/10.1016/j.conbuildmat.2015.10.192

738 Filho, J.R.T., de Araújo, M.A.P.G., Snoeck, D., De Belie, N., 2019. Discussing different approaches for
739 the time-zero as start for autogenous shrinkage in cement pastes containing superabsorbent
740 polymers. Materials (Basel). 12. https://doi.org/10.3390/ma12182962

741 G.J. Al-Sulaimani, M. Kaleemullah, L.A. Basunbul, et al. Influence of corrosion and cracking on bond
742 behaviour and strength of reinforced concrete members ACI Struct. J., 87 (2) (1990), pp. 220-
743 231, n.d.

744 G.P. Tilly, J.J., 2007. Concrete Repairs, Performance in Service and Current Practice. Bracknell.

745 Gontia, P., Janssen, M., 2016. Life cycle assessment of bio-based sodium polyacrylate production
746 from pulp mill side streams: Case study of thermo-mechanical and sulfite pulp mills. J. Clean.
747 Prod. 131, 475–484. https://doi.org/10.1016/j.jclepro.2016.04.155

748 Gruyaert, E., Debbaut, B., Snoeck, D., Díaz, P., Arizo, A., Tziviloglou, E., Schlangen, E., De Belie, N.,
749 2016. Self-healing mortar with pH-sensitive superabsorbent polymers: Testing of the sealing
750 efficiency by water flow tests. Smart Mater. Struct. 25. https://doi.org/10.1088/0964-
751 1726/25/8/084007

752 J. Piérard, V. Pollet, and N.C., n.d. International RILEM Conference on Volume Changes of Hardening

753 Concrete: Testing and Mitigation. 2006. Lyngby, Denmark: RILEM Publications SARL.

754 J.S. Williamson, L.A. Clark Pressure required to cause cover cracking of concrete due to
755 reinforcement corrosion Mag. Concr. Res., 52 (6) (2000), pp. 455-467, n.d.

756 L.A. Clark, M. Saifullah, Effect of corrosion on reinforcement bond strength, in: M. Forde (Ed.),
757 Proceedings of 5th International Conference on Structural Faults and Repairs, Edinburgh:
758 Engineering Technical Press, vol. 3, 1993, pp. 113–119, n.d.

759 Liu, J., Farzadnia, N., Khayat, K.H., Shi, C., 2021. Effects of SAP characteristics on internal curing of
760 UHPC matrix. Constr. Build. Mater. 280. https://doi.org/10.1016/j.conbuildmat.2021.122530

761 Liu, Y., Presuel-Moreno, F.J., Paredes, M.A., 2015. Determination of chloride diffusion coefficients in
762 concrete by electrical resistivity method. ACI Mater. J. 112, 631–640.
763 https://doi.org/10.14359/51687777

764 Luca Bertolini, Bernhard Elsener, Pietro Pedeferri, R.P.P., 2004. Corrosion of steel in concrete.

765 Mechtcherine, V. and H.W.R., n.d. Application of Super Absorbent Polymers (SAP) in Concrete
766 Construction, in State-of-the-Art Report Prepared by Technical Committee 225-SAP. 2012,
767 RILEM. p. 165.

768 Meyer, C., 2009. The greening of the concrete industry. Cem. Concr. Compos. 31, 601–605.
769 https://doi.org/10.1016/j.cemconcomp.2008.12.010

770 Noh, H.M., Idris, N., Noor, N., Sarpin, N., 2018. Structural Effects of Reinforced Concrete Beam Due to
771 Corrosion 01024, 1–9.

772 Pelto, J., Leivo, M., Gruyaert, E., Debbaut, B., Snoeck, D., De Belie, N., 2017. Application of
773 encapsulated superabsorbent polymers in cementitious materials for stimulated autogenous
774 healing. Smart Mater. Struct. 26. https://doi.org/10.1088/1361-665X/aa8497

775 Plank, J., Sakai, E., Miao, C.W., Yu, C., Hong, J.X., 2015. Chemical admixtures - Chemistry, applications
776 and their impact on concrete microstructure and durability. Cem. Concr. Res. 78, 81–99.
777 https://doi.org/10.1016/j.cemconres.2015.05.016

778 Provveditorato interregionale per la Lombardia e l'Emilia Romagna, 2021. PREZZARIO REGIONALE
779 delle opere pubbliche. https://www.regione.lombardia.it/wps/wcm/connect/52c6917f-cb22-
780 4aa9-8018
781 bf7ebd0ca118/C%29+Prezzario+2021+VOLUME_2_1.pdf?MOD=AJPERES&CACHEID=ROOTWOR
782 KSPACE-52c6917f-cb22-4aa9-8018-bf7ebd0ca118-nrz6KQ4. (Accessed 25th October 2021)

783 Regione Emilia Romagna, 2011. CARTA DELLA SALINITA' DEI SUOLI DELLA PIANURA EMILIANO-
784 ROMAGNOLA STRATO 50-100 cm.

785 S. Rasheeduzzafar, S.S. Al-Saadoun, A.S. Al-Gahtani Corrosion cracking in relation to bar diameter and
786 concrete quality J. Mater. Civ. Eng., 4 (4) (1992), pp. 327-342, n.d.

787 Schmid, Jay–Epoxy or Polyurethane Foam, Waterproof! Magazine, Spring, 2010 Available online at
788 www.waterproofmag.com, n.d.

789 Shafikhani, M., Chidiac, S.E., 2019. Quantification of concrete chloride diffusion coefficient – A critical
790 review. Cem. Concr. Compos. 99, 225–250. https://doi.org/10.1016/j.cemconcomp.2019.03.011

791 SIKA–Waterproofing-Solutions for Water Seal, using SIKA Injection Systems in Concrete, Masonry and
792 Natural Stone Structures (in Portuguese). SIKA Brazil Marketing Catalog. Available online at
793 http://bra.sika.com (September 2015)., n.d.

794 Snoeck, D., Roigé, N., Manso, S., Debbaut, B., Segura, I. & De Belie, N. (2021). The effect of (recycled)

superabsorbent polymers on the water retention capability and bio-receptivity of cementitious materials. Resources, Conservation & Recycling, submitt, n.d.

Snoeck, D., 2015. Self-healing and microstructure of cementitious materials with microfibres and superabsorbent polymers. Ghent University.

Snoeck, D., Jensen, O.M., De Belie, N., 2015. The influence of superabsorbent polymers on the autogenous shrinkage properties of cement pastes with supplementary cementitious materials. Cem. Concr. Res. 74, 59–67. https://doi.org/10.1016/j.cemconres.2015.03.020

Snoeck, D., Steuperaert, S., Van Tittelboom, K., Dubruel, P., De Belie, N., 2012. Visualization of water penetration in cementitious materials with superabsorbent polymers by means of neutron radiography. Cem. Concr. Res. 42, 1113–1121. https://doi.org/10.1016/j.cemconres.2012.05.005

Snoeck, D., Van Tittelboom, K., Steuperaert, S., Dubruel, P., De Belie, N., 2014. Self-healing cementitious materials by the combination of microfibres and superabsorbent polymers. J. Intell. Mater. Syst. Struct. 25, 13–24. https://doi.org/10.1177/1045389X12438623

Tenório Filho, J. R., Mannekens, E., Van Tittelboom, K., Van Vlierberghe,S., De Belie, N., Snoeck, D. 2021a. "Innovative SuperAbsorbent Polymers (iSAPs) to construct crack-free reinforced concrete walls: An in-field large-scale testing campaign." Journal of Building Engineering 43: 102639. https://doi.org/10.1016/j.jobe.2021.102639

Tenório Filho, J. R., Vermoesen, E., Mannekens, E., Van Tittelboom, K., Van Vlierberghe, S., De Belie, N., & Snoeck, D., 2021b. Enhanced durability performance of cracked and uncracked concrete by means of smart in-house developed superabsorbent polymers with alkali-stable and -unstable crosslinkers. CONSTRUCTION AND BUILDING MATERIALS, 297. https://doi.org/10.1016/j.conbuildmat.2021.123812.

Tenório Filho, J.R., Mannekens, E., Van Tittelboom, K., Snoeck, D., De Belie, N., 2020a. Assessment of the potential of superabsorbent polymers as internal curing agents in concrete by means of optical fiber sensors. Constr. Build. Mater. 238. https://doi.org/10.1016/j.conbuildmat.2019.117751

Tenório Filho, J.R., Snoeck, D., De Belie, N., 2020b. Mixing protocols for plant-scale production of concrete with superabsorbent polymers. Struct. Concr. 21, 983–991. https://doi.org/10.1002/suco.201900443

Torres-Acosta, A.A., Presuel-Moreno, F.J., Andrade, C., 2019. Electrical resistivity as durability index for concrete structures. ACI Mater. J. 116, 245–253. https://doi.org/10.14359/51718057

UNI, 2015. UNI EN ISO 16627:2015 - Sustainability of construction works - Assessment of economic performance of buildings - Calculation methods.

UNI, 2021a. UNI EN ISO 14040:2021, Environmental management - Life cycle assessment - Principles and framework.

UNI, 2021b. UNI EN ISO 14044:2021, Environmental management - Life cycle assessment - Requirements and guidelines.

UNI, 2019. UNI EN 15804:2019, Sustainability of construction works - Environmental product declarations - Core rules for the product category of construction products.

Van Belleghem, B., 2018. Effect of Capsule-Based Self-Healing on Chloride Induced Corrosion of Reinforced Concrete. Ghent University.

Van den Heede, P., Mignon, A., Habert, G., De Belie, N., 2018. Cradle-to-gate life cycle assessment of

self-healing engineered cementitious composite with in-house developed (semi-)synthetic superabsorbent polymers. Cem. Concr. Compos. 94, 166–180. https://doi.org/10.1016/j.cemconcomp.2018.08.017

Y. Liu, R.E. Weyers Modelling the time-to-corrosion cracking in chloride contaminated reinforced concrete structures ACI Mater. J., 95 (6) (1998), pp. 675-681, n.d.

Zhang, X., Zhang, Y., Liu, Bin, Liu, Bowen, Wu, W., Yang, C., 2021. Corrosion-induced spalling of concrete cover and its effects on shear strength of RC beams. Eng. Fail. Anal. 127, 105538. https://doi.org/10.1016/j.engfailanal.2021.105538